

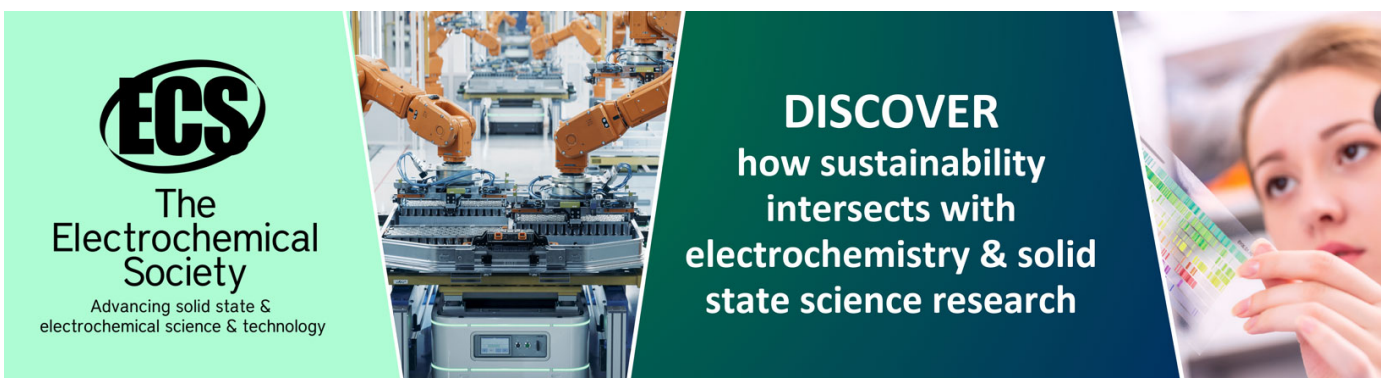
## Analytic signal extraction approach based on 2D Grating Interferometer and systematic comparison between 2D GI and 1D case

To cite this article: Z. Ju *et al* 2016 *JINST* 11 C03031

View the [article online](#) for updates and enhancements.

### You may also like

- [Plasmonic wideband and tunable absorber based on semi etalon nano structure in the visible region](#)  
N Roostaei, H Mbarak, S Almasi Monfared et al.
- [Analysis of period and visibility of dual phase grating interferometer](#)  
Jun Yang, , Jian-Heng Huang et al.
- [Infrared plasmonic refractive index sensor utilizing 2D grating of nano-bowtie particles for both gas and liquid](#)  
Xiangxian Wang, Xijun Rao, Jiankai Zhu et al.



**ECS**  
The  
Electrochemical  
Society  
Advancing solid state &  
electrochemical science & technology

**DISCOVER**  
how sustainability  
intersects with  
electrochemistry & solid  
state science research

RECEIVED: November 14, 2015

REVISED: January 14, 2016

ACCEPTED: February 9, 2016

PUBLISHED: March 15, 2016

SYMPOSIUM ON MULTI-SCALE AND MULTI-DIMENSIONAL SYNCHROTRON RADIATION  
IMAGING TECHNIQUES AND APPLICATIONS  
3–6 Nov. 2015  
SHANGHAI, P.R. CHINA

## Analytic signal extraction approach based on 2D Grating Interferometer and systematic comparison between 2D GI and 1D case

Z. Ju,<sup>a</sup> Y. Wang,<sup>a</sup> P. Li,<sup>a</sup> Z. Zhu,<sup>a</sup> K. Zhang,<sup>a</sup> W. Huang,<sup>a</sup> Q. Yuan,<sup>a,1</sup> Z. Wu<sup>b</sup> and P. Zhu<sup>a,1</sup>

<sup>a</sup>*Institute of High Energy Physics, Chinese Academy of Science,  
Yuquan Road, Beijing, People's Republic of China*

<sup>b</sup>*National Synchrotron Radiation Laboratory, University of Science and Technology of China,  
Hefei, People's Republic of China*

*E-mail:* [yuanqx@ihep.ac.cn](mailto:yuanqx@ihep.ac.cn), [Zhupp@ihep.ac.cn](mailto:Zhupp@ihep.ac.cn)

**ABSTRACT:** X-ray imaging method based on 2D grating interferometer was proposed and studied recently, to overcome the limitations in signal extraction and phase retrieval when using 1D grating interferometer. In this paper, the concept of angle-signal response function is proposed, and different surfaces of different 2D setups under the condition of parallel coherent light are calculated and depicted with Matlab. Based on this concept, performance of 2D grating interferometer is systematically analyzed and an analytic 2D signal extraction approach is theoretically proposed. Besides, signal extraction, phase retrieval and feasibility of using conventional source are also briefly discussed and compared between 2D grating interferometer and 1D case.

**KEYWORDS:** Interferometry; Image reconstruction in medical imaging; Medical-image reconstruction methods and algorithms, computer-aided diagnosis

---

<sup>1</sup>Corresponding author.

---

## Contents

<b>1</b>	<b>Introduction</b>	<b>1</b>
<b>2</b>	<b>Method</b>	<b>2</b>
2.1	Angle-signal response surface	2
2.2	Moving along one direction	6
2.3	Moving along two directions	8
<b>3</b>	<b>Comparison and discussion</b>	<b>9</b>
<b>4</b>	<b>Conclusion</b>	<b>10</b>

---

## 1 Introduction

For non-destructive inspection and substantially increased contrast of weak absorption materials, various phase-sensitive rather than attenuation-sensitive X-ray imaging methods were developed in the past decades, such as interferometric methods [1–3], free-space propagation methods [4–6] and techniques using analyzer crystal [7–10]. Grating Interferometry(GI) is a new phase-contrast imaging method that has been developed over the past few years [11–14]. GI is highly sensitive to subtle deviations of wave front direction, which is a typical kind of angle signal imaging method and supplies differential phase contrast. Compared with other methods, GI has been demonstrated that it doesn't need a high degree of X-ray monochromaticity and spatial coherence, thus can work not only on synchrotron facilities but also with conventional X-ray tubes, which gives a prospect of clinical application [15].

The standard GI method widely discussed hitherto is focusing on 1D case, which consists of two specifically developed line gratings placed one behind the other. The first one is a phase-shifting line grating, acts as a beam splitter, the second one is an absorbing grating, and often referred to as analyzer. However, using interferometer of this kind, we can only get angle signals perpendicular to grating lines, angle signals parallel to the lines are not visible. Furthermore, phase retrieval of the wave front can't be perfectly fulfilled due to lack of information in the blind direction. To overcome these limitations, 2D GI method based on 2D gratings was proposed and studied recently [16–18]. As reported, 2D angle signals were extracted, quantitative phase maps were retrieved without artifacts using 2D GI set-up.

The same as 1D GI's history, the original signal extraction method used in 2D GI is also the so-called phase stepping (PS) [14] technique, in which multiple images are acquired and a first-order approximation of the Fourier series of the transmission function is applied to extract absorption and differential phase signals. Here we theoretically propose an analytic signal extraction approach alternative to the conventional PS procedure, which is inspired by Diffraction Enhanced

Imaging (DEI) [8] algorithm in analyzer based imaging method and the Reverse Projection [20] method in 1D GI.

To establish the whole analytic signal extraction approach in this paper, first we propose the concept of angle-signal response surface, and show different surfaces in commonly used 2D GI setups. Based on angle-signal response surface, we then systematically analyze when moving analyzer grating along one and two directions respectively, what signals can be extracted and show the algorithms.

Besides, till now we focused on 2D GI, but are there essential advantages of 2D GI, can we use 1D GI to realize the same effect with equivalent experimental operation haven't been carefully discussed. So in the third section we briefly make comparisons in signal extraction, phase retrieval and feasibility to use conventional x-ray source aspects between 2D GI and 1D case, then give the conclusion of this paper.

## 2 Method

### 2.1 Angle-signal response surface

The same as 1D case, basic physical principle of 2D GI is also Talbot effect, which is also known as self-image effect [12–19].

In 1D case, we define duty cycle as  $\gamma = w/p$ , where  $w$  is the grating line width,  $p$  is the grating period, and we commonly preferred duty cycle  $\gamma = 0.5$  for both beam splitter and analyzer grating. Here in 2D case, we only discuss gratings with fourfold symmetry, and  $\gamma_x = \gamma_y = 0.5$ . Two of the simplest unit cells are what we henceforward refer to as checkerboard (CB-) and mesh (M-) type patterns.

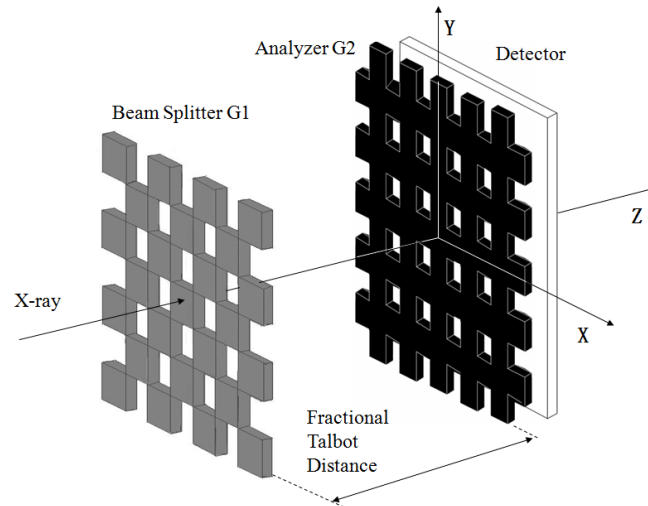


**Figure 1.** Schematic of imaging setup based on 2D grating interferometer.

We take the setup schematically shown in figure 1 for example. It consists of a fixed positioned CB-type  $\pi$ -shifting phase grating G1 whose self image is mesh type as beam splitter, a movable M-type absorption grating G2 whose period and duty cycle are exactly the same as the self image and placed at one of the fractional talbot distances of G1 as analyzer, and a detector fixed right behind G2.

Without sample, when G2 moves relatively to the self image of G1 along every possible direction in x-y plane, there will be corresponding intensity change in the detector and thus forming an intensity surface in every pixel. When the sample is added right before or after G1 in the beam, due to refraction in the sample, local self image of G1 will be distorted and thus deflected relative to G2 along two transverse directions. The deflection will be analyzed by G2 and then converted into intensity variations in the detector. By analyzing variations of the intensity in every pixel, we can extract signals of the sample.

The same as DEI method, in which the change of included angle between the analyzer crystal and the monochromator crystal is equivalent to the refraction angle of the sample, in GI method, the influence of refraction angle of the sample is equivalent to that caused by relative movement between G2 and G1. Considering the equivalence and taking the whole 2D GI setup as a system, refraction in different points of the sample can be seen as angle-signal, and the intensity surface recorded by the detector when there is no sample can be called angle-signal response surface or angle-signal response function now. In DEI, there is concept of rocking curve [8–10] and correspondingly shifting curve in 1D GI [20], they are another two kinds of angle-signal response functions. Together with the surfaces in 2D GI, they are all inherent attributes of the imaging system.

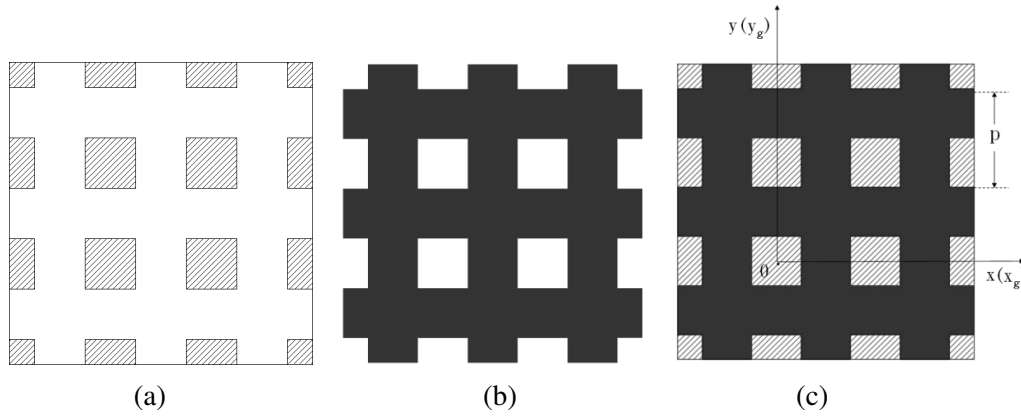


**Figure 2.** Position relationship between self image and analyzer grating. (a) Self image of grating G1; (b) M-type analyzer grating G2; (c) Position relationship between self image and G2.

Here we consider the condition of parallel coherent light, or partial coherent light whose transverse coherent length can cover at least one period of G1. In realistic situation, we should also consider the influence of source size and detector response, here we ignore these factors for simplification. We define intensity of the self image of G1 as  $I_s$  whose peak value is  $I_p$ , the transmission function of G2 as  $T$ , relative movement of the self image as  $x_g$  and  $y_g$  as shown in figure 2. Then we can write:

$$I_s(x, y) = \begin{cases} I_p, & \left(-\frac{p}{4} + \xi p \leq x \leq \frac{p}{4} + \xi p, -\frac{p}{4} + \eta p \leq y \leq \frac{p}{4} + \eta p, \xi, \eta \in Z\right) \\ 0, & \text{(Others)} \end{cases} \quad (2.1)$$

$$T(x, y) = \begin{cases} 1, & \left(-\frac{p}{4} + \xi p \leq x \leq \frac{p}{4} + \xi p, -\frac{p}{4} + \eta p \leq y \leq \frac{p}{4} + \eta p, \xi, \eta \in Z\right) \\ 0, & \text{(Others)} \end{cases} \quad (2.2)$$

In commonly used GI setups, there are usually several self image stripes in one pixel, so the intensity recorded by every pixel is an average value. As  $I_s$  and  $T$  are both periodic functions, without sample the intensity  $I$  recorded by the detector can be written by:

$$I(x, y, x_g, y_g) = \frac{1}{p^2} \iint_{\substack{x - \frac{p}{4}, x + \frac{3p}{4} \\ y - \frac{p}{4}, y + \frac{3p}{4}}} I_s(x, y) T(x - x_g, y - y_g) dx dy = I(x_g, y_g) \quad (2.3)$$

which means, without sample, every pixel's intensity is the same, having no relationship with the pixel's position, only decided by relative movement between G1 and G2. Calculating and normalizing  $I(x_g, y_g)$ , we can get the angle-signal response function:

$$S_1(x_g, y_g) = \left[ 1 - \frac{2|x_g - n_1 p|}{p} \right] \left[ 1 - \frac{2|y_g - n_2 p|}{p} \right] \quad (2.4)$$

$$\left( |x_g - n_1 p| \leq \frac{p}{2}, |y_g - n_2 p| \leq \frac{p}{2}, n_1, n_2 \in \mathbb{Z} \right)$$

So far, there are four kinds of 2D GI setup units commonly discussed as shown in figure 3 [21], and we find out there are only three kinds of angle-signal response surfaces in them.

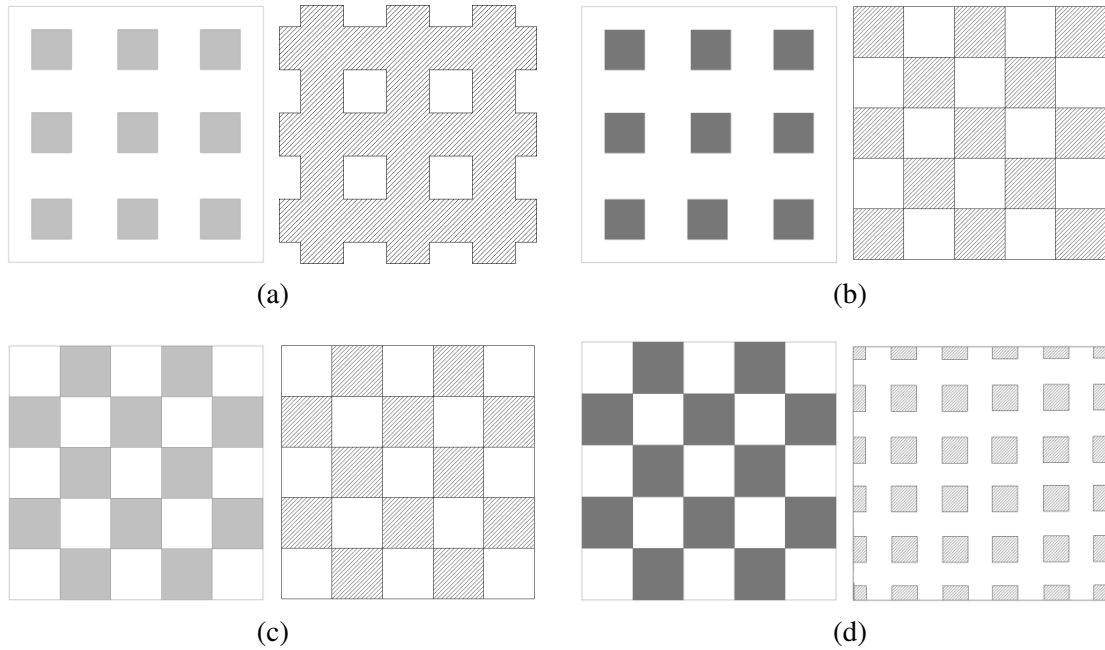


**Figure 3.** Commonly discussed 2D GI setup units. All units, phase grating is in left, self image is in right. In phase grating, white for no phase shifting, light gray for  $\pi/2$ , dark gray for  $\pi$ -shifting. In self image, shadow for self image stripe white for no light. (a) M-type  $\pi/2$ -shifting phase grating and its M-type self image; (b) M-type  $\pi$ -shifting phase grating and CB-type self image; (c) CB-type  $\pi/2$ -shifting phase grating and CB-type self image; (d) CB-type  $\pi$ -shifting phase grating and anti-M-type self image.

For case (d) in figure 3, we have already get the result in eq. (2.4). And for case (b) and (c), based on the similar analysis, we can get:

$$S_2(x_g, y_g) = 1 - \frac{2(|x_g - n_1p| + |y_g - n_2p|)}{p} + \frac{8|x_g - n_1p||y_g - n_2p|}{p^2}$$

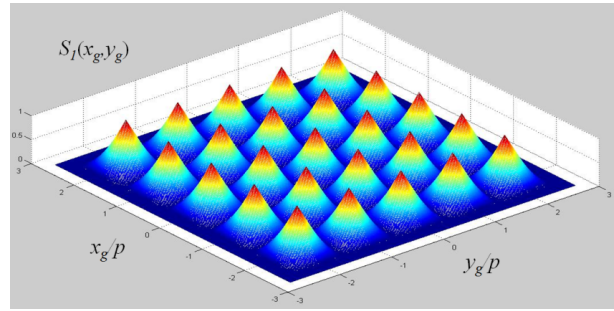
$$|x_g - n_1p| \leq \frac{p}{2}, \quad |y_g - n_2p| \leq \frac{p}{2}, \quad n_1, n_2 \in Z \quad (2.5)$$

For case (a), we can get:

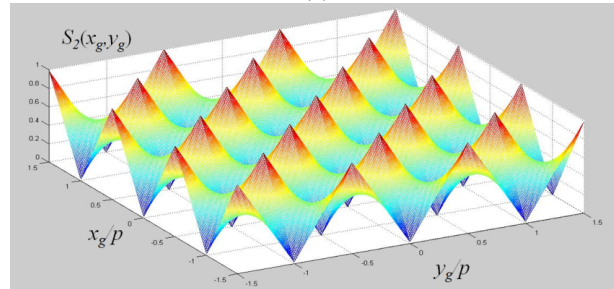
$$S_3(x_g, y_g) = \frac{2}{p} \cdot (|x_g - n_1p| + |y_g - n_2p|) - \frac{4|x_g - n_1p||y_g - n_2p|}{p^2}$$

$$|x_g - n_1p| \leq \frac{p}{2}, \quad |y_g - n_2p| \leq \frac{p}{2}, \quad n_1, n_2 \in Z \quad (2.6)$$

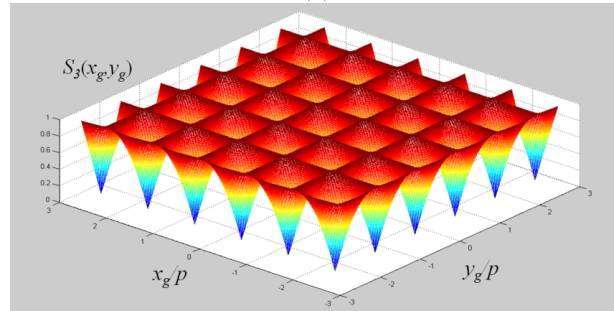
Here we also show the shape of the angle-signal response surfaces in figure 4.



(a)



(b)



(c)

**Figure 4.** Angle-signal Response Surfaces. (a) Surface depicted by formula (2.4); (b) Surface depicted by formula (2.5); (c) Surface depicted by formula (2.6).

## 2.2 Moving along one direction

There are many paths that we can move G2 along. However, in practice we usually choose the line ones, such as  $0^\circ$ ,  $90^\circ$ ,  $45^\circ$  and  $135^\circ$ . We still take the setup shown in figure 1 as example. The figure of its angle-signal response surface in one period is shown in figure 5(a), four commonly used paths have been drawn in its contour as in figure 5(b). Moving along these paths, we can get angle-signal response curves, which we can also call shifting curves.

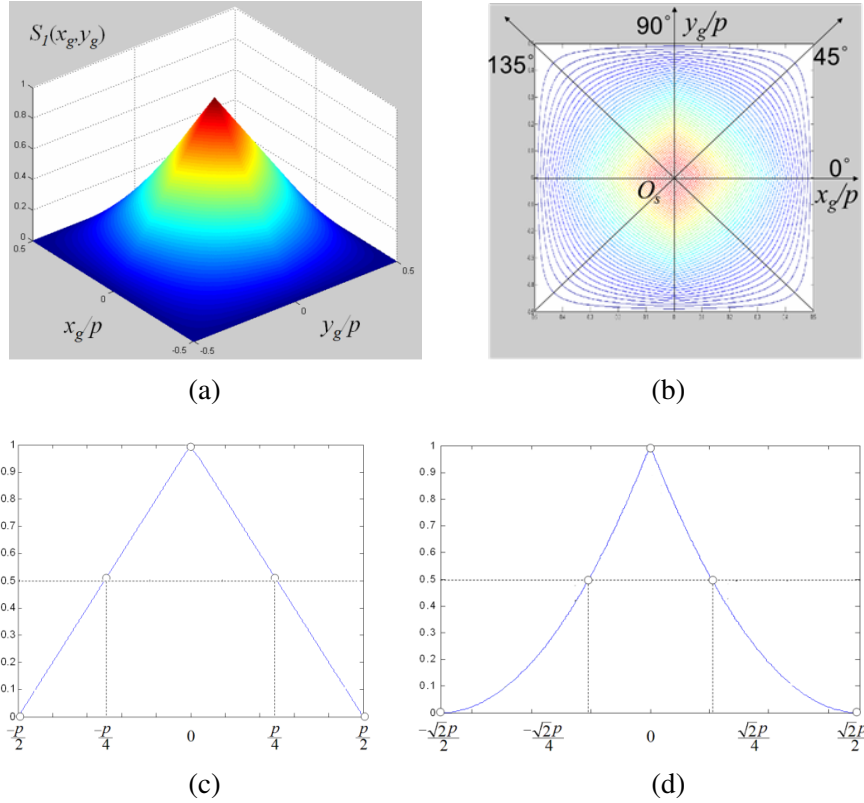


**Figure 5.** Angle-signal Response Surface and its curves. (a) Angle-signal Response Surfaces  $S_1$  in one period; (b) Four commonly used paths shown in its contour; (c) Shifting curve moving along  $0^\circ$  or  $90^\circ$ ; (d) Shifting curve moving along  $45^\circ$  or  $135^\circ$ .

From eq. (2.4), we can get the  $0^\circ$  shifting curve as:

$$S_x(x_g) = 1 - \frac{2|x_g|}{p}, \quad |x_g| \leq \frac{p}{2} \quad (2.7)$$

the  $90^\circ$  shifting curve as:

$$S_y(y_g) = 1 - \frac{2|y_g|}{p}, \quad |y_g| \leq \frac{p}{2} \quad (2.8)$$

and the  $45^\circ$  or  $135^\circ$  shifting curves as:

$$S_l(l) = S_1(x_g, y_g) = \left(1 - \frac{\sqrt{2}|l|}{p}\right)^2, \quad |l| = \sqrt{2}|x_g| = \sqrt{2}|y_g| \leq \frac{p}{\sqrt{2}} \quad (2.9)$$

The shapes of eq. (2.7), (2.8) and (2.9) have been shown in figure 5(c) and (d).

As an object is placed right before or after G1, the incident x-rays will not only be attenuated but also refracted and scattered, and the interference pattern will be distorted from its reference shape. For simplicity, in this paper we focus on the absorption and refraction signals. When moving the analyzer grating along a certain direction, the intensity recorded by the detector can be expressed as:

$$I(x, y) = I_0 \cdot \exp[-M(x, y)] \cdot S_l[l + D\theta_l(x, y)] \quad (2.10)$$

where  $I_0$  is the incident intensity before G1,  $M(x, y) = \int \mu(x, y, z) dz$  represents the sample's absorption,  $\mu$  is the linear absorption coefficient,  $D$  is the Fractional Talbot distance between G1 and G2, and  $\theta_l$  is the refraction angle of the sample along the direction of the shifting curve.

When moving along  $0^\circ$  or  $90^\circ$ , we find that the expression and figure of 2D GI shifting curve are exactly the same with 1D GI as in figure5(c), which means when moving along these two directions respectively, 2D GI can be used just like 1D case, only capable of getting the sample's refraction angle  $\theta_x$  along x-axis or  $\theta_y$  along y-axis each time.

For figure 5(d), moving along  $45^\circ$  or  $135^\circ$ , we take two images setting the analyzer grating G2 at up half-slope where  $l^u = (1 - \sqrt{2})p/2$  and down half-slope where  $l^d = (\sqrt{2} - 1)p/2$  respectively. Then we can write the intensity as:

$$I^u(x, y) = I_0 \cdot \exp[-M(x, y)] \cdot S_l[l^u + D\theta_l(x, y)] \quad (2.11)$$

$$I^d(x, y) = I_0 \cdot \exp[-M(x, y)] \cdot S_l[l^d + D\theta_l(x, y)] \quad (2.12)$$

For small values of  $\theta_l$ ,  $S_l[l + D\theta_l(x, y)]$  can be replaced by a first-order Taylor expansion,

$$S_l[l + D\theta_l(x, y)] = S_l(l) + \frac{dS_l(l)}{dl} D\theta_l(x, y) = S_l(l) [1 + C\theta_l(x, y)] \quad (2.13)$$

where

$$C = \frac{\frac{dS_l(l)}{dl} D}{S_l(l)}, \quad S_l(l^u) = S_l(l^d) \quad (2.14)$$

Taking eq. (2.13) into eq. (2.11) and (2.12), we can get:

$$I^u(x, y) = I_0 \cdot \exp[-M(x, y)] \cdot S_l(l^u) [1 + C\theta_l(x, y)] \quad (2.15)$$

$$I^d(x, y) = I_0 \cdot \exp[-M(x, y)] \cdot S_l(l^d) [1 - C\theta_l(x, y)] \quad (2.16)$$

Combining eq. (2.9), (2.14)–(2.16), we can get absorption and refraction angle of the sample:

$$M(x, y) = \ln\left(\frac{I_0}{I^u(x, y) + I^d(x, y)}\right) \quad (2.17)$$

$$\theta_l(x, y) = \frac{p}{2} \cdot \frac{I^u(x, y) - I^d(x, y)}{I^u(x, y) + I^d(x, y)} \quad (2.18)$$

$\theta_l$  is the refraction angle along  $45^\circ$  or  $135^\circ$ . Considering  $0^\circ$  and  $90^\circ$  case together, we find that moving 2D analyzer grating along one direction, we can only extract 1D angle signals. As we have already known the relationship between refraction angle and phase shift  $\Phi$ ,

$$\theta_l(x, y) = \frac{\lambda}{2\pi} \frac{\partial \Phi(x, y)}{\partial l} = - \int \frac{\partial \delta(x, y, z)}{\partial l} dz \quad (2.19)$$

where  $\delta$  is the decrement of the real part of the refractive index of the object, in fact moving G2 along any line direction  $l$ , we can only calculate the directional derivative along  $l$  direction, which is 1D information.

### 2.3 Moving along two directions

We still take the surface depicted by formula (2.4) for example. When moving along two directions, usually we choose simple orthogonal directions, such as  $0^\circ$  and  $90^\circ$  or  $45^\circ$  and  $135^\circ$ . In this paper we choose the later case for discussion.

Similarly with eq. (2.10), when a sample is placed right before or after G1, the intensity recorded by the detector can be written as:

$$I(x, y) = I_0 \cdot \exp[-M(x, y)] \cdot S_1[x_g + D\theta_x(x, y), y_g + D\theta_y(x, y)] \quad (2.20)$$

where

$$\theta_x = \frac{\lambda}{2\pi} \frac{\partial \Phi(x, y)}{\partial x}, \quad \theta_y = \frac{\lambda}{2\pi} \frac{\partial \Phi(x, y)}{\partial y} \quad (2.21)$$

As we have already figured out the angle-signal response surface  $S_1$  in former section, and there are only three unknown parameters  $M$ ,  $\theta_x$ ,  $\theta_y$  in eq. (2.20), we propose the analytic method of taking three images to extract absorption and two dimensional refraction signals, which decreases the amount of images required by PS method.

Setting G2 at three positions respectively where the relative displacements are  $(-p/4, -p/4)$ ,  $(p/4, p/4)$  and  $(p/4, -p/4)$  as shown in figure 6, three images  $I_1$ ,  $I_2$  and  $I_3$  are acquired.

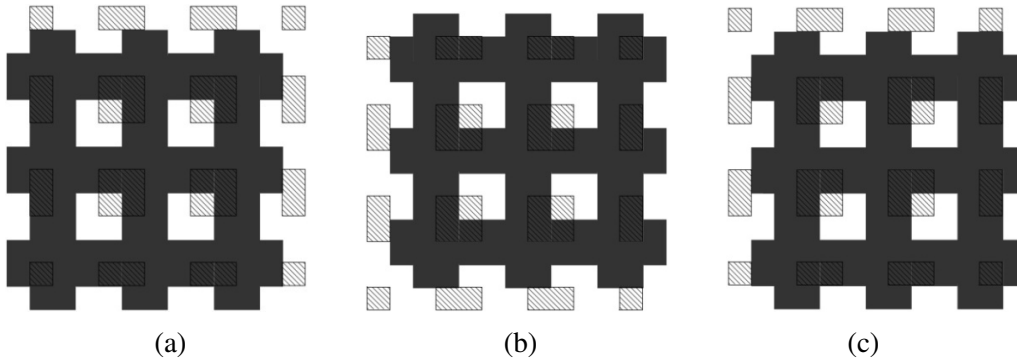


**Figure 6.** Position relationship between self image and analyzer grating. The shadow stripe for self image, the black stripe for analyzer grating G2. (a) relative displacement  $(-p/4, -p/4)$ ; (b) relative displacement  $(p/4, p/4)$ ; (c) relative displacement  $(p/4, -p/4)$ .

Taking the three coordinates into eq. (2.4) and (2.20), we can write:

$$I_1 = I_0 \exp(-M) \left( \frac{1}{2} + \frac{2D\theta_x}{p} \right) \left( \frac{1}{2} + \frac{2D\theta_y}{p} \right) \quad (2.22)$$

$$I_2 = I_0 \exp(-M) \left( \frac{1}{2} - \frac{2D\theta_x}{p} \right) \left( \frac{1}{2} - \frac{2D\theta_y}{p} \right) \quad (2.23)$$

$$I_3 = I_0 \exp(-M) \left( \frac{1}{2} - \frac{2D\theta_x}{p} \right) \left( \frac{1}{2} + \frac{2D\theta_y}{p} \right) \quad (2.24)$$

Combining eq. (2.22), (2.23) and (2.24), we can get the absorption signal:

$$M = \ln \left[ \frac{I_0 \cdot I_3}{(I_1 + I_3)(I_2 + I_3)} \right] \quad (2.25)$$

the horizontal and vertical refraction angle:

$$\theta_x = \frac{p}{4D} \cdot \frac{I_1 - I_3}{I_1 + I_3}, \quad \theta_y = \frac{p}{4D} \cdot \frac{I_3 - I_2}{I_3 + I_2} \quad (2.26)$$

Considering the length, in this paper we've only taken  $S_1$  for instance and discussed carefully, for the other two angle-signal response surfaces  $S_2$  and  $S_3$ , similar analysis can be made based on the same thoughts.

### 3 Comparison and discussion

Till now we focused on 2D GI's advantages. It can extract 2D refraction signals, overcoming the limitation of 1D GI in which we can only get angle signal perpendicular to the grating lines and blind in the other direction. However, we can also use 1D GI setup to get 2D refraction signals through either PS [22] or other analytic signal extraction approaches by rotating the sample or the 1D gratings in x-y plane.

In 1D case whose analyzer grating's period is also  $p$ , see figure 7, first we set the 1D analyzer grating at up half-slope where  $x_g^u = -p/4$  and down half-slope where  $x_g^d = p/4$  respectively, take two images  $I'_1$  and  $I'_2$ , then turn the sample for  $90^\circ$ , which is equivalent with turning the gratings, set analyzer at up half-slope of y-axis where  $y_g^u = -p/4$ , then take the images  $I'_3$ .

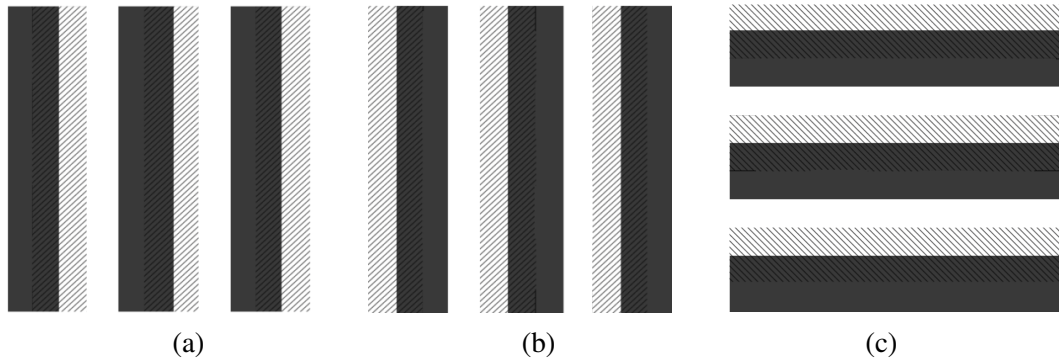


**Figure 7.** Position relationship between self image and analyzer grating. The shadow stripe for self image of 1D beam splitter, the black stripe for analyzer grating G2. (a) relative displacement  $x_g^u = -p/4$ ; (b) relative displacement  $x_g^d = p/4$ ; (c) relative displacement  $y_g^u = -p/4$ .

Then we can get three equations:

$$I'_1(x, y) = I_0 \cdot \exp[-M(x, y)] \cdot S_x \left[ x_g^u + D\theta_x(x, y) \right] \quad (3.1)$$

$$I'_2(x, y) = I_0 \cdot \exp[-M(x, y)] \cdot S_x \left[ x_g^d + D\theta_x(x, y) \right] \quad (3.2)$$

$$I'_3(x, y) = I_0 \cdot \exp[-M(x, y)] \cdot S_y \left[ y_g^u + D\theta_y(x, y) \right] \quad (3.3)$$

where  $S_x$  and  $S_y$  are actually the same. Combining eq. (2.7), (2.8), (3.1), (3.2)–(3.3), we can get:

$$M = \ln \left( \frac{I_0}{I'_1 + I'_2} \right), \quad \theta_x = \frac{p}{4D} \cdot \frac{I'_1 - I'_2}{I'_1 + I'_2}, \quad \theta_y = \frac{p}{4D} \cdot \frac{2I'_3 - I'_1 - I'_2}{I'_1 + I'_2} \quad (3.4)$$

We can see, to get absorption and two dimensional refraction signals through the analytic signal extraction approach we proposed, 2D GI and 1D both need three images. Although 1D GI needs to add one more set of mechanical rotating device, it has higher diffraction efficiency than 2D GI, and the fabrication and alignment of 2D GI are also more complicated.

Phase retrieval aspect was also considered as another important advantage of 2D GI [18]. In 1D case, due to not only lack of exact boundary values of phase, but also affected by noise in the phase gradient images, strong stripe artifacts show up in retrieved phase image. However, as long as we can get 2D signals, we can take retrieval algorithm based on Fourier analysis to make the final phase map smooth enough without stripe artifacts [22]. As we can use 1D GI to analytically get 2D signals by rotating, phase retrieval aspect should not be essential advantage of 2D GI.

Being able to implement on conventional x-ray source [15] thus having the potential of clinic practice is a very important feature of GI compared to other methods. But as the source grating and analyzing grating are both absorbing gratings, if we develop two dimensional Talbot-Lau-type imaging interferometer, see figure 8, the luminous flux of source x-ray will be reduced by at least 4 times relative to 1D case and flux of analyzer grating will be 1/2 of that in 1D case. This means to get the same exposure dose, 2D setup needs much more time than 1D case and thus will have much lower signal-to-noise ratio. So 1D GI even has advantage in this aspect.

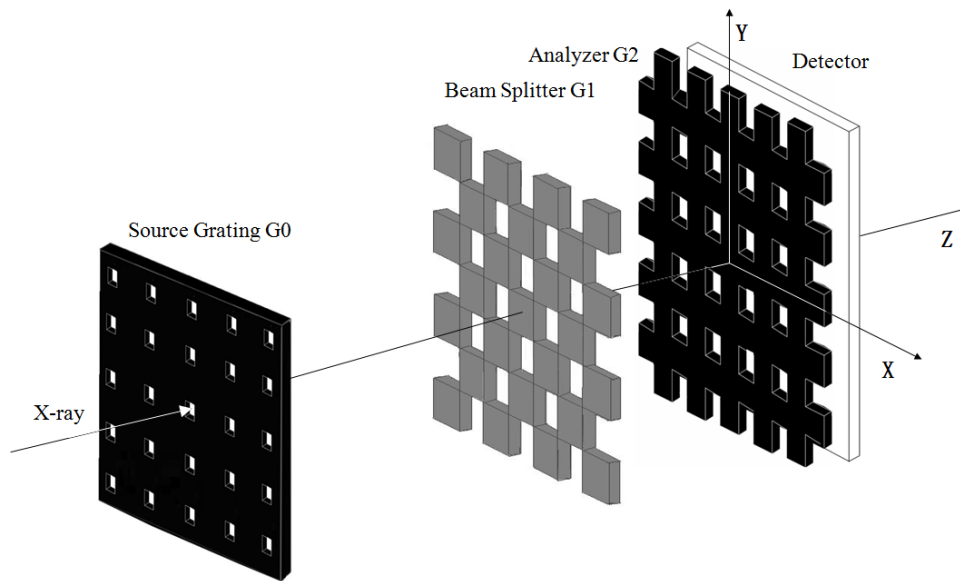


**Figure 8.** Schematic 2D Talbot-Lau Grating Interferometry setup.

#### 4 Conclusion

In this paper, we proposed the concept of angle-signal response surface and calculated different cases. Based on this concept, we systematically analyzed the signal extraction approach of 2D GI. We found when moving along one direction, 2D GI can only extract one dimensional refraction signal, which is the directional derivative of phase shift; when moving along two directions, we theoretically proposed the analytic approach to extract two dimensional refraction signals.

At last we also systematically and briefly compared 2D GI with 1D case from signal extraction, phase retrieval and feasibility to use conventional x-ray source aspects, and gave corresponding 2D signals extraction method using 1D GI. We approve the development of 2D GI, and we also believe the quality and potential of 1D GI, especially in the aspect of implementing on conventional x-ray source.

## Acknowledgments

This project is supported by the National Basic Research Program of China (Grant No. 2012CB8258 00), the National Natural Science Foundation of China (Grant No. 11205189, 11375225 and U1332109), and the Knowledge Innovation Program of the Chinese Academy of Science (KJ CX2-YW-N42).

## References

- [1] U. Bonse et al., *An X-ray interferometer*, *Appl. Phys. Lett.* **6** (1965) 155.
- [2] M. Ando et al., *An attempt at x-ray phase-contrast microscopy*, in *Proceedings of 6th International Conference On Xray Optics and Microanalysis*, G. Shinoda, K. Kohra and T. Ichinokawa eds., University of Tokyo Press, Tokyo Japan (1972), pg. 63.
- [3] A. Momose, *Demonstration of phase-contrast X-ray computed tomography using an X-ray interferometer*, *Nucl. Instrum. Meth. A* **352** (1995) 622.
- [4] A. Snigirev et al., *On the possibilities of x-ray phase contrast microimaging by coherent high-energy synchrotron radiation*, *Rev. Sci. Instrum.* **66** (1995) 54865.
- [5] S.W. Wilkins et al., *Phase-contrast imaging using polychromatic hard X-rays*, *Nature* **384** (1996) 335.
- [6] K.A. Nugent et al., *Quantitative Phase Imaging Using Hard X Rays*, *Phys. Rev. Lett.* **77** (2006) 2961.
- [7] T.J. Davis et al., *Phase-contrast imaging of weakly absorbing materials using hard X-rays*, *Nature* **373** (2005) 595.
- [8] D. Chapman et al., *Diffraction enhanced x-ray imaging*, *Phys. Med. Biol.* **42** (1997) 2015.
- [9] Z. Zhong et al., *Implementation of diffraction-enhanced imaging experiments at the nsls and aps*, *Nucl. Instrum. Meth. A* **45** (1997) 556.
- [10] P.P. Zhu et al., *Diffraction enhanced imaging: a simple model*, *J. Phys. D* **39** (2006) 4142.
- [11] C. David et al., *Differential x-ray phase contrast imaging using a shearing interferometer*, *Appl. Phys. Lett.* **81** (2002) 3287.
- [12] A. Momose et al., *Demonstration of X-Ray Talbot interferometry*, *Jpn. J. Appl. Phys.* **42** (2003) L866.
- [13] T. Weitkamp et al., *X-ray wavefront analysis and optics characterization with a grating interferometer*, *Appl. Phys. Lett.* **86** (2005) 054101.
- [14] T. Weitkamp et al., *X-ray phase imaging with a grating interferometer*, *Opt. Express* **13** (2005) 6296.
- [15] F. Pfeiffer et al., *Phase retrieval and differential phase-contrast imaging with low-brilliance X-ray sources*, *Nature Phys.* **2** (2006) 258.
- [16] A. Momose et al., *X-ray Talbot Interferometry with Capillary Plates*, *Jpn. J. Appl. Phys.* **45** (2006) 314.

- [17] A. Olivo et al., *A non-free-space propagation x-ray phase contrast imaging method sensitive to phase effects in two directions simultaneously*, *Appl. Phys. Lett.* **94** (2009) 044108.
- [18] I. Zanette et al., *Two-Dimensional X-Ray Grating Interferometer*, *Phys. Rev. Lett.* **105** (2010) 248102.
- [19] P. Cloetens et al., *Fractional Talbot imaging of phase gratings with hard x rays*, *Optics Lett.* **22** (1997) 1059.
- [20] P.P. Zhu et al., *Low-dose, simple, and fast grating-based X-ray phase-contrast imaging*, *Proc. Natl. Acad. Sci.* **107** (2010) 13576.
- [21] I. Zanette et al., *2D grating simulation for X-ray phase-contrast and dark-field imaging with a Talbot interferometer*, at *20th International Congress on X-Ray Optics and Microanalysis*, Karlsruhe Germany, 15–17 September 2009.
- [22] C. Kottler et al., *A two-directional approach for grating based differential phase contrast imaging using hard x-rays*, *Opt. Express* **15** (2007) 1175.